Physica A 484 (2017) 282–298

Contents lists available at ScienceDirect

Physica A

journal homepage: www.elsevier.com/locate/physa

High pressures in room evacuation processes and a first approach to the dynamics around unconscious pedestrians

F.E. Cornes [a], G.A. Frank [c,*], C.O. Dorso [a,b]

[a] Departamento de Física, Facultad de Ciencias Exactas y Naturales, Universidad de Buenos Aires, Pabellón I, Ciudad Universitaria, 1428 Buenos Aires, Argentina

[b] Instituto de Física de Buenos Aires, Pabellón I, Ciudad Universitaria, 1428 Buenos Aires, Argentina

[c] Unidad de Investigación y Desarrollo de las Ingenierías, Universidad Tecnológica Nacional, Facultad Regional Buenos Aires, Av. Medrano 951, 1179 Buenos Aires, Argentina

HIGHLIGHTS

- High pressures during an emergency evacuation may produce unconsciousness.
- Dodging or passing-through the fallen individuals changes the evacuation performance.
- Dodging worsens the evacuation performance depending on the anxiety levels of the pedestrians.
- Passing-through enhances the evacuation depending on the difficulties to be surmounted.

ARTICLE INFO

Article history:
Received 18 January 2017
Received in revised form 2 May 2017
Available online 10 May 2017

Keywords:
Emergency evacuation
Social force model
Unconscious pedestrians

ABSTRACT

Clogging raises as the principal phenomenon during many evacuation processes of pedestrians in an emergency situation. As people push to escape from danger, compression forces may increase to harming levels. Many individuals might fall down, while others will try to dodge the fallen people, or, simply pass through them. We studied the dynamics of the crowd for these situations, in the context of the "social force model". We modeled the unconscious (fallen) pedestrians as inanimate bodies that can be dodged (or not) by the surrounding individuals. We found that new morphological structures appear along the evacuating crowd. Under specific conditions, these structures may enhance the evacuation performance. The pedestrian's willings for either dodging or passing through the unconscious individuals play a relevant role in the overall evacuation performance.

1. Introduction

History acknowledges many fatalities during stampedes. Unfortunately, such kind of disasters have increased in frequency because the number and size of massive events (music festivals, sports events, etc.) has become larger [1]. An inspection of the Crowdsafe Database™ through 1992–2002 shows a correlation between the number of concerts and festival events, and the number of injuries [2]. Specially sorrowful are the incidents occurred in the nightclubs *The Station* (Rhode Island, 2003) and *Cromañón* (Buenos Aires, 2004) where 100 and 194 people lost their lives, respectively.

Laboratory experiments and numerical simulations provide some guidelines for a better understanding of these kind of disasters [3]. The exit width raises as one of the major reasons for overcrowding during evacuation processes [4,5]. It has

* Corresponding author.
E-mail address: frank@ieee.org (G.A. Frank).

http://dx.doi.org/10.1016/j.physa.2017.05.013
0378-4371/

been pointed out, however, that other behavioral patterns or environmental conditions are responsible for clogging just before any narrowing of the leaving pathway [3,6–8]. Researchers agree on the fact that pathways as narrow as 0.6–0.7 m reduce the capacity of the pedestrians to leave the room [9,10].

The overcrowding is one of the principal causes of injury or death while people try to escape during crowd disaster. Deaths may happen because of *trampling* or *compression due to crush*. The former occurs when someone falls in a high dense crowd, not being able to stand again due to the movement of the others, unaware of the fallen pedestrian. This produces a continue trampling that finally kills the individual [11].

Compression due to crush is the other cause of death. This effect appears in high dense crowds, preventing the free movement of the pedestrians. If the pressures in the crowd become extremely high, each time an individual breaths out, the pressure restricts the inhalation of the next breath. Thus, compression due to crush causes asphyxia on the individual, evolving to unconsciousness or death after some time [12]. Further information on fatal consequences by asphyxia can be found in Ref. [11].

A brief review of the basic "social force model" can be found in Section 2.1. We include in Section 2.2 an upgrade of the basic model that makes possible to achieve compressional injuries.

In Section 3 we will present experimental data on the injury threshold due to compression. A simple model on the human torso will be examined for further simulations (see Section 4).

All the results of our investigations are presented in Section 5. The corresponding conclusions are summarized in Section 6.

2. Background

2.1. The social force model

The "social force model" (SFM) proposed by Helbing and co-workers [13] is a generalized force model, including socio-psychological forces, as well as "physical" forces like friction. These forces enter the Newton equation as follows.

$$m_i \frac{d\mathbf{v}^{(i)}}{dt} = \mathbf{f}_d^{(i)} + \sum_{j=1}^{N} \mathbf{f}_s^{(ij)} + \sum_{j=1}^{N} \mathbf{f}_g^{(ij)} \tag{1}$$

where the i, j subscripts correspond to any pedestrian in the crowd. $\mathbf{v}^{(i)}(t)$ means the current velocity of the pedestrian (i), while $\mathbf{f}_d$ and $\mathbf{f}_s$ are the socio-psychological forces acting on him (her). $\mathbf{f}_g$ is the friction or granular force.

$\mathbf{f}_d(t)$ and $\mathbf{f}_s(t)$ are essentially different. The former corresponds to the "desire force", that is, the pedestrians own willings to move towards a desired position. The latter corresponds to the "social force", meaning the tendency of the pedestrians to preserve their *private sphere*. The "social force" prevents the pedestrians from getting too close to each other.

According to the anxiety state of the pedestrian, he (she) will accelerate (or decelerate) to reach any desired velocity v_d that will make him (her) feel more comfortable. Thus, in the social force model, the desired force reads [13]

$$\mathbf{f}_d^{(i)}(t) = m_i \frac{v_d^{(i)}\, \mathbf{e}_d^{(i)}(t) - \mathbf{v}^{(i)}(t)}{\tau} \tag{2}$$

where m_i is the mass of the pedestrian i and τ represents the relaxation time needed to reach his (her) desired velocity. $\mathbf{e}_d$ is the unit vector pointing to the target position. For simplicity, we assume that v_d remains constant during an evacuation process, but $\mathbf{e}_d$ changes according to the current position of the pedestrian. Detailed values for m_i and τ can be found in Refs. [13,14].

The *private sphere* preservation corresponds to a repulsive feeling between the pedestrians, or, between pedestrians and the walls [13,15]. These repulsive feelings become stronger as people get closer to each other (or to the walls). Thus, in the context of the social force model, this tendency is expressed as

$$\mathbf{f}_s^{(ij)} = A_i\, e^{(r_{ij}-d_{ij})/B_i} \mathbf{n}_{ij} \tag{3}$$

where (ij) represents any pedestrian–pedestrian pair, or pedestrian–wall pair. A_i and B_i are two fixed parameters (see Ref. [16]). The distance $r_{ij} = r_i + r_j$ is the sum of the pedestrians radius, while d_{ij} is the distance between the center of mass of the pedestrians i and j. $\mathbf{n}_{ij}$ means the unit vector in the $\vec{ji}$ direction. For the case of repulsive feelings with the walls, d_{ij} corresponds to the shortest distance between the pedestrian and the wall, while $r_{ij} = r_i$ [13,15].

The granular force $\mathbf{f}_g$ included in Eq. (1) corresponds to the sliding friction between pedestrians in contact, or, between pedestrians in contact with the walls. The expression for this force is

$$\mathbf{f}_g^{(ij)} = \kappa\, (r_{ij} - d_{ij})\, \Theta(r_{ij} - d_{ij})\, \Delta\mathbf{v}^{(ij)} \cdot \mathbf{t}_{ij} \tag{4}$$

where κ is a fixed parameter. The function $\Theta(r_{ij} - d_{ij})$ is zero when its argument is negative (that is, $r_{ij} < d_{ij}$) and equals unity for any other case (Heaviside function). $\Delta\mathbf{v}^{(ij)} \cdot \mathbf{t}_{ij}$ represents the difference between the tangential velocities of the sliding bodies (or between the individual and the walls).

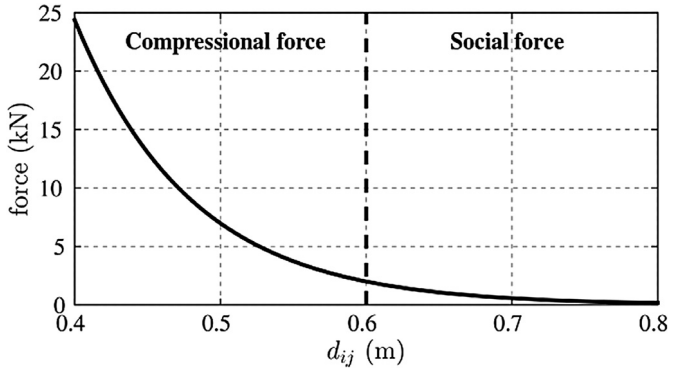

Fig. 1. Labeling associated to the social force ($\mathbf{f}_s$) as a function of the inter-pedestrian distance d_{ij}. The dashed line at 0.6 m corresponds to the meeting distance between the compression label ($\mathbf{f}_c$) and the social one ($\mathbf{f}_s$).

2.2. Body compression in the social force model

The social force expressed in Eq. (3) attains some kind of body compression for $d_{ij} < r_{ij}$. Thus, it surpasses the "private sphere" preservation, while it might trigger pain or injury upon contacting pedestrians.

The force $\mathbf{f}_s^{(ij)}$ actuates no matter if the neighboring pedestrians are in contact or not (cfr. Refs. [13,16]). But, since it involves body compression for the contacting distances $d_{ij} < r_{ij}$, we choose to label the social force as a "compression" force for the contacting situation. The corresponding mathematical expressions read as follows

$$\begin{cases} \mathbf{f}_c^{(ij)} = A_i e^{(r_{ij}-d_{ij})/B_i} \mathbf{n}_{ij}\, \Theta[r_{ij}-d_{ij}] \\ \mathbf{f}_s^{(ij)} = A_i e^{(r_{ij}-d_{ij})/B_i} \mathbf{n}_{ij}\, \Theta[d_{ij}-r_{ij}] \end{cases} \tag{5}$$

where Θ is the Heaviside function. We stress the fact that Eqs. (5) refer to the same force but expressed in a piecewise form. The $\mathbf{f}_c^{(ij)}$ label accounts for the body compression associated to distances $d_{ij} < r_{ij}$ (see Fig. 1).

Although the expressions in Eqs. (5) correspond to the same force, we will refer to "compression force" or "social force" as a token for the respective domain. Notice, however, that the movement Eq. (1) needs no further modification because of this.

In order to capture the physical meaning of the compressional force $\mathbf{f}_c^{(ij)}$, we expand the expression in (5) into powers of $r_{ij} - d_{ij}$ (within the domain $r_{ij} > d_{ij}$). The first order terms are as follows

$$\mathbf{f}_c^{(ij)} = A_i\, \mathbf{n}_{ij} + \frac{A_i}{B_i}\,(r_{ij}-d_{ij})\,\mathbf{n}_{ij} + \mathcal{O}[(r_{ij}-d_{ij})^2]\,\mathbf{n}_{ij}. \tag{6}$$

The first term on the right $A_i\,\mathbf{n}_{ij}$ corresponds to the repulsive feelings at $d_{ij} = r_{ij}$. The second term on the right resembles the Hooke law with elastic coefficient A_i/B_i. This law applies to small body compressions. The third term on the right, however, resembles the stiffness for large compressions. According to literature values, the elastic coefficient A_i/B_i is 25 000 N/m (see Refs. [13,14]). In Section 3 we will show that this value is in agreement with experimental data for small body compressions.

We want to stress the fact that $\mathbf{f}_c^{(ij)}$, as expressed in Eq. (5), corresponds to an untested hypothesis for large compressions. Literature data actually show that there exists a non-linear relation between $r_{ij} - d_{ij}$ and $\mathbf{f}_c^{(ij)}$ for large compressions (see Refs. [17,18]), but no precise relations are currently available, to our knowledge. Thus, Eq. (5) should be considered as a *first approach* to the high pressure scenario.

2.3. The effective compressional force

We are interested in the forces causing body deformation in the front–back direction. This are actually the forces that may cause injury to the pedestrians. Therefore, we define the following "effective" compressional force

$$f_e^{(i)} = \sum_{j\neq i}^{N} \left| (\mathbf{f}_c^{(ij)} - A_i \mathbf{n}_{ij}) \cdot \mathbf{e}_d^{(i)} \right| \Theta[r_{ij}-d_{ij}] \tag{7}$$

where $A_i\,\mathbf{n}_{ij}$ is the repulsive feeling at the contacting distance $d_{ij} = r_{ij}$. The inner product produces the projection of the compressional force (excluding the repulsive feelings at $d_{ij} = r_{ij}$) in the front–back direction. The bars means the modulus of the magnitude. The sum does not include the walls, since we assume that the desired direction $\mathbf{e}_d^{(i)}$ is tangential to the walls surface.

2.4. The local pressure on the pedestrians

The "social pressure" on a single pedestrian (say, i) is [13]

$$p^{(i)} = \frac{1}{2\pi r_i} \sum_{j \neq i}^{N} [\mathbf{f}_s^{(ij)} + \mathbf{f}_c^{(ij)}] \cdot \mathbf{n}_{ij}. \tag{8}$$

The sum $\mathbf{f}_s^{(ij)} + \mathbf{f}_c^{(ij)}$ does not overlap, while it ensures continuity at $d_{ij} = r_{ij}$. Recall that both forces point from any individual j to the individual i, and thus, the inner product is always positive.

Notice that Eq. (8) holds either if the pedestrians are in contact or not. The feelings for preserving the *private sphere* actuate as a "social pressure" that makes possible for the individuals to change their behavioral pattern when they come too close to each other or to the walls. The compressional force also changes the moving pattern of the pedestrian, if two pedestrians get in contact.

2.5. The pass through force

Pedestrians are capable of passing through other fallen individuals. This situation, however, cannot be achieved by the basic "social force model" (SFM). According to Section 2.1, repulsive feelings (*i.e.* the social force) actuate on neighboring pedestrians. Only the individual's own desire (*i.e.* desire force) can balance these feelings because the granular force is actually orthogonal to the inter-pedestrian direction. Therefore, it might happen that, although the pedestrian wants to accelerate towards the target position, he (she) will get stuck because of repulsion.

The dynamics for passing through fallen individuals require further extensions of the basic SFM. The relevant force acting on the moving pedestrian during this process is his (her) desire to "pass through" the fallen individual. We postulate as a *working hypothesis* that a force actuates during the "passing through" process that is similar to the desire force $\mathbf{f}_d^{(i)}$, as follows

$$\mathbf{f}_p^{(i)}(t) = m_i \frac{v_p^{(i)} \mathbf{e}_p^{(i)}(t) - \mathbf{v}_i(t)}{\tau'} \tag{9}$$

where v_p represents a "desired passing through" velocity, $\mathbf{e}_p$ is the corresponding passing through direction and τ' is the relaxation time of the moving individual during the "passing through" process. The "desired passing through" velocity v_p should be less than v_d since it represents the slowing down with respect to v_d due to the additional difficulties of the "passing through" context. The passing through direction $\mathbf{e}_p$, however, is the same as the desired velocity ($\mathbf{e}_p^{(i)} = \mathbf{e}_d^{(i)}$) since passing through fallen individuals can only take place if the latter is in the same path as the former.

Notice that $\mathbf{f}_d^{(i)}$ and $\mathbf{f}_p^{(i)}$ do not overlap in time. That is, the "passing through" force replaces the usual desired force whenever the moving pedestrian is in contact with the fallen pedestrian. This means that Eq. (1) needs no further modification.

2.6. Clustering structures

Clusterization is responsible for the time delays during an evacuation process, as explained in Refs. [16,19]. Thus, a definition for the clustering structures appearing during an evacuation process is required. We define a *human cluster* as the group of pedestrians that for any member of the group (say, i) there exists at least another member belonging to the same group (j) in contact with the former. That is,

$$i \in \mathcal{G} \Leftrightarrow \exists j \in \mathcal{G} / d_{ij} < r_i + r_j \tag{10}$$

where $\mathcal{G}$ corresponds to any set of individuals.

One or more human clusters may be responsible for blocking the way out of the room. The minimum set of human clusters that are able to block the way out of the room will be called *blocking clusters*. If only one human cluster exists, we will call this blocking situation as a *total blocking*. If more than one human cluster exists simultaneously, we will call this situation a *partial blocking*.

3. Experimental data for model parameters

It was mentioned in Section 1 that compression due to crush may cause unconsciousness or death in an overcrowded environment. During an emergency, where people push hard to get out, compression due to neighboring pedestrians can raise above certain injury limit. Although it is not possible to determine empirically this limit, a lower bound for the true injury level can still be established from the corresponding pain threshold.

Table 1 resumes typical parameter values for the human body. Force thresholds were measured for quasi-static situations (that is, impact velocities less than 1 m/s). The elastic coefficients result from data fitting procedures into the (linear) Hooke's law. For further details see Ref. [20].

Table 1
Experimental data for human body compression. Surface figures correspond to mean human values. The tolerance threshold was measured on the abdomen or sternum of the individuals, and lasted 1 s, according to Ref. [21]. The death threshold corresponds to forces applied on the chest during 15 s. The elastic coefficients on the sternum correspond to deflections smaller than 25 and 38 mm, respectively. The elastic coefficient on the thorax corresponds to deflections smaller than 41 mm.

Magnitude	Symbol	Value	Units	Refs.
Mean body surface	S_B	1.750	m^2	[22]
Mean torso surface	S_T	0.068	m^2	[20,23]
Force tolerance threshold	F_T	276–356	N	[21]
Force death threshold	F_D	6227	N	[24]
Elastic coefficient on sternum	k_s	13.1–21.9	kN/m	[20]
Elastic coefficient on thorax	k_t	26.2	kN/m	[20]

Data shown in Table 1 focuses on the front–back direction. Body compression on the chest is, indeed, the relevant one since it restricts inhalation on each breathing cycle. Forces applied on the left–right sides of the body do not play an important role for human survivability (see Ref. [12]). Notice that the "effective" compressional force defined in Section 2.3 resembles the chest compression only.

According to Table 1, the thorax seems to be somehow stiffer than the sternum. But, the upper bound for the sternum elastic coefficient k_s is quite similar to the one for the thorax, and both are close to the estimation 25 kN/m, obtained in Section 2.2. Thus, the compressional force in Section 2.2 is in agreement with the experimental data.

The forces F_T and F_D exhibited in Table 1 correspond to two different measurement conditions. The tolerance threshold F_T represents the pain limit when pressure is applied during 1 s on the abdomen or sternum area. The death threshold represents the limit of fatality when pressure is applied during 15 s on the chest area. The total amount $15 \times F_T$ is less than F_D since pain occurs at an early stage before injury. We choose the F_D value as a suitable estimation for the falling pressure in our model. This pressure is approximately $6227\ \text{N}/0.068\ \text{m}^2 = 91.6\ \text{kN/m}^2$.

The ratio between the torso surface and the body surface is $S_T/S_B = 0.039$, according to Table 1. This is the fraction of the human body where the pressure limit of $91.6\ \text{kN/m}^2$ is applied to (during 15 s). We will assume that this fraction remains approximately valid, regardless of the volume representation of the body. That is, for any chosen body model (*i.e.* sphere, cylinder) enclosed by a surface S, we will assume that the piece of surface $0.039 \times S$ corresponds to an "effective" torso surface. The compressional pressure is supposed to be applied on this area.

In order to link the experimental data shown in Table 1 to the model parameters, we associate the pressure limit $91.6\ \text{kN/m}^2$ to the "effective" compressional force defined in Section 2.3. That is, we postulate that the "effective" force limit for reaching unconsciousness or fatality is roughly

$$f_e^{\max} = 91.6 \times 0.039 \times S. \tag{11}$$

The surface S needs to be specified for achieving a numerical value of $f_e^{\max}$. This value will be computed in Section 4.2.

4. Numerical simulations

4.1. Boundary and initial conditions

We simulated the evacuation process of 225 pedestrians from a 20 m × 20 m room with a single exit door. The door width was $L = 1.2$ m, enough to allow up to two pedestrians to escape simultaneously.

The process started with all the pedestrians inside the room and equally separated in a square arrangement, as shown in the Fig. 2. The occupancy density was set to 0.6 people/m^2, as suggested by healthy indoor environmental regulations [25]. The pedestrians had random initial velocities computed from a Gaussian distribution (with null mean value). The rms value for the Gaussian distribution was close to 1 m/s.

The desired velocity v_d was the same for all the individuals, meaning that all of them had the same anxiety level. At each time-step, however, the desired direction $\mathbf{e}_d$ was updated, in order to point to the exit.

The evacuation processes began with all the pedestrians moving randomly, but willing to go to the exit. If certain conditions were met (see Section 4.2), any moving pedestrian could switch his (her) behavior to the "fallen" pedestrian behavior. Fallen pedestrians were those that remained at a fix position.

The evacuation processes were implemented on the LAMMPS molecular dynamics simulator [26]. LAMMPS was set to run on multiple processors. The chosen time integration scheme was the velocity Verlet algorithm with a time step of 10^{-4} s. Any other parameter was the same as in previous works (see Refs. [7,14]).

We simulated between 30 and 360 processes for each evacuation situation (see figures caption for details). Data was recorded at time intervals of 0.05 s. The processes lasted for 300 s, but a few situations were also examined until 800 s (see Section 5.1.1 for details). Only the evacuation processes shown in Section 5.2 lasted until 100 individuals were able to leave the room.

The explored anxiety levels ranged from relaxed situations ($v_d < 1$ m/s) to highly stressing ones ($v_d = 8$ m/s). Recall that the "faster is slower" effect occurs within this range.

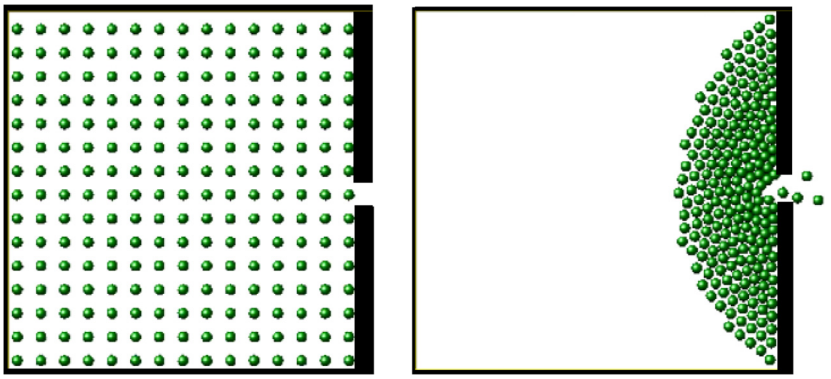

(a) Initial state. (b) State at 10 s.

Fig. 2. Snapshots of an evacuation process from a 20 m × 20 m room with a single door for 225 pedestrians. The picture on the left represents the initial configuration. The picture on the right represents the evacuation process after 10 s. All the individuals correspond to "moving pedestrians". The black lines represents the walls. The desired velocity was $v_d = 6$ m/s.

4.2. Moving and fallen pedestrians

We separated the pedestrians behavioral patterns into two categories: "moving" individuals and "fallen" individuals. The former are those that move according to Eq. (1). The latter are those that are not able to move at all until the end of the evacuation process. Moving pedestrians, however, can switch to the fallen category, but fallen pedestrians always remain in that category.

The condition for a moving pedestrian to switch to a fallen pedestrian's behavior is that the compressional pressure actuating on him (her) reaches the unconsciousness (or fatality) threshold for an uninterrupted time period of at least 15 s (see Section 3). This threshold is expressed by Eq. (11). We simply modeled the pedestrian's body as spheres of radius $r_i = 0.3$ m (roughly, the neck-shoulder distance) and surface $S = 4\pi r_i^2 = 1.13\,\text{m}^2$. Therefore, the compressional threshold, in our model, became $f_e^{\max} = 4030$ N.

During the evacuation process simulation, we computed the "effective" force f_e actuating on each moving pedestrian. This value was accumulated along time in a discrete variable z_i as follows

$$z_i = \begin{cases} z_i + 1 & \text{if} \quad f_e \geq f_e^{\max} \\ z_i & \text{if} \quad 0 < f_e < f_e^{\max} \\ 0 & \text{if} \quad f_e = 0 \end{cases} \tag{12}$$

where z_i was set to zero at the beginning of the process for each pedestrian i. Notice that the z_i value is reseted whenever the "effective" compressional force f_e vanishes, since the pedestrian's breathing restrictions are supposed to be released. The condition for the moving pedestrian i to become unconscious (*i.e.* "fallen" pedestrian) is that $z_i = 300$. Recall that the data recording was done every 0.05 s, and thus, the $z_i = 300$ threshold represents a time period of 15 s since 300×0.05 s $= 15$ s.

Any meeting situation between a moving pedestrian and a fallen one was handled in two possible ways: the moving pedestrian dodged the fallen pedestrian (similar to an obstacle avoidance), or, the moving pedestrian passed through the fallen one. The dodging scenario is examined from Sections 5.1.1–5.1.4, while the passing-through scenario is examined in Section 5.2.

In the dodging scenario, the forces actuating on the moving pedestrian due to the fallen individual were similar to the forces actuating between two neighboring moving pedestrians. That is, the moving pedestrian experienced the same repulsive feelings and sliding friction as if the fallen individual belonged to the "moving" category. In the passing-through scenario, neither repulsive feelings nor friction (due to the fallen individual) were present on the moving pedestrian. But, as explained in Section 2.5, the desired force $\mathbf{f}_d$ was replaced by the "passing-through" force $\mathbf{f}_p$. The rest of the forces between moving pedestrians remained the same.

Recall that the "passing-through" scenario corresponds to a first approach on this kind of behavioral patterns. Therefore, we want to stress the fact that our model is as simple as we could imagine, in order to study the most basic effects out of the zero order approach of avoiding fallen pedestrians.

5. Results

We divided our investigation into two different scenarios. From Sections 5.1.1–5.1.4 we examined those situations where the moving pedestrians were only able to dodge the fallen individuals. In Section 5.2 we relaxed this restriction, while allowing the moving pedestrians to pass-through the fallen individuals. A new *working hypothesis* was introduced to achieve this behavioral pattern. Finally, in Section 5.2 we compared the results obtained from these two main scenarios.

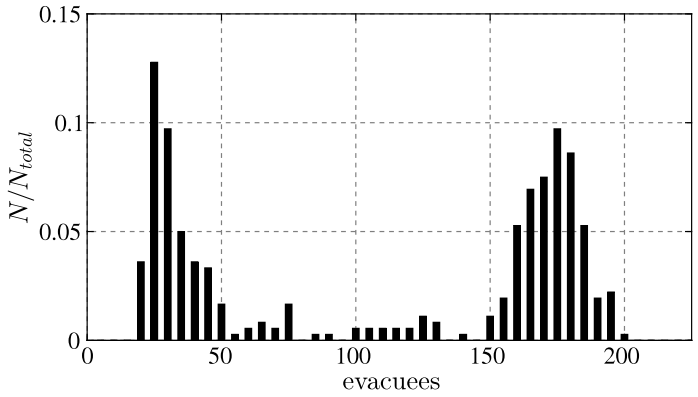

Fig. 3. Normalized distribution of evacuees during the first 300 s. We considered bins of five pedestrians between the range of 0–200 individuals. N is the number of events corresponding to each bin. The plot is normalized with respect to the total number of events. Data was recorded from 360 evacuation processes. The desired velocity was $v_d = 6$ m/s.

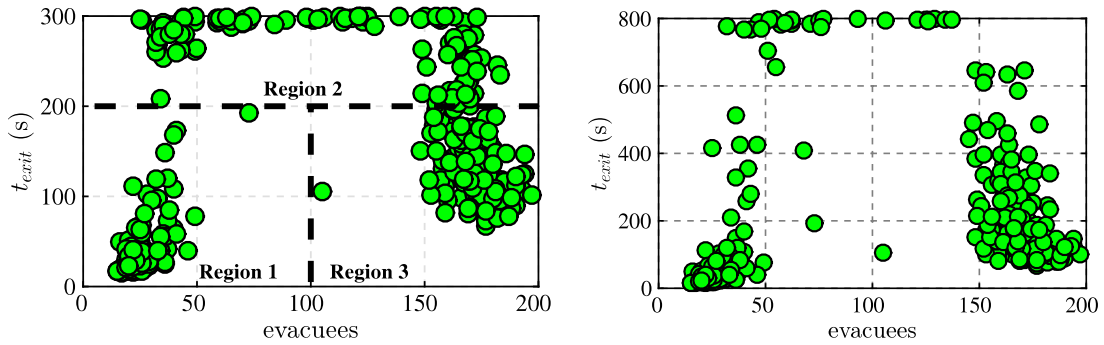

(a) Time window of 300 s.

(b) Time window of 800 s.

Fig. 4. Outgoing time t_{exit} of the last evacuee (before 300 s on the left and 800 s on the right) as a function of the number of evacuees. Each circle represents an evacuation process. 360 processes are exhibited in the plot. The dashed lines represents a qualitative boundary for three regions, labeled as "region 1", "region 2" and "region 3". The desired velocity was $v_d = 6$ m/s.

5.1. The dodging scenario

We first examined the evacuation processes at the desired velocity of 6 m/s in order to achieve the "faster is slower" effect. In Section 5.1.4 we varied the desired velocity from a relaxed situation to a highly stressing one.

5.1.1. The outgoing flux at high pressure levels for the dodging scenario

Fig. 3 shows the histogram for the evacuees distribution during the first 300 s of the leaving process (see caption for details). As can be seen, the most probable number of evacuees lies within two separated intervals: the lower interval ranging between 0 and 50 evacuees, and the upper interval ranging between 150 and 200 evacuees. The intermediate interval in between, say, 50–150 evacuees is very unlikely.

In order to get a better understanding of the evacuation process, we inspected each process during a time window of 300 and 800 s. We recorded the time when the last pedestrian left the room for each process. Fig. 4(a) shows the recorded time t_{exit} vs. the number of pedestrians that left the room for the 300 s case. Likewise, Fig. 4(b) shows the recorded time t_{exit} for the 800 s case.

The data points in Fig. 4(a) show that the number of leaving pedestrians mostly lie in the lower and upper intervals, as exhibited in Fig. 3. But, the leaving time for the last pedestrian t_{exit} (before 300 s) usually does not exceed 200 s. We can envisage some kind of correlation between the leaving time for the last individual (before 300 s) and the total number of evacuees.

Notice in Fig. 4(a) that t_{exit} is close to 300 s for the number of leaving pedestrians that lie between 50 and 150 individuals. The crosscheck with the recording at 800 s shows that many of the data points that formerly lied in the 50–150 evacuee interval (see Fig. 4(a)), actually move to the upper interval (beyond 150 evacuees) in Fig. 4(b). This means that the 50–150 evacuee interval corresponds to not completely finished processes, and consequently, to a "slowing down" in the evacuation.

Fig. 4(a) summarizes three qualitative situations. These are roughly separated by the dashed lines. The first situation (labeled as "region 1") corresponds to those processes where a small fraction of the pedestrians are able to leave the room and the evacuation virtually ceases after 200 s. The second situation (labeled as "region 2") corresponds to a "slowing down"

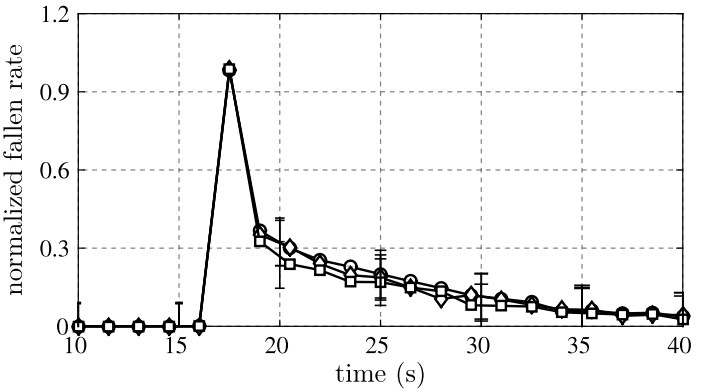

Fig. 5. Normalized fallen rate vs. time (in seconds). ◯ represent the "region 1" processes. ◊ represent the "region 2" processes. □ represent the "region 3" processes. Mean values were computed from (approx.) 120 realizations. The curves are normalized to have its maximum at unity. The error bars corresponds to $\pm\sigma$ (one standard deviation). The desired velocity was $v_d = 6$ m/s.

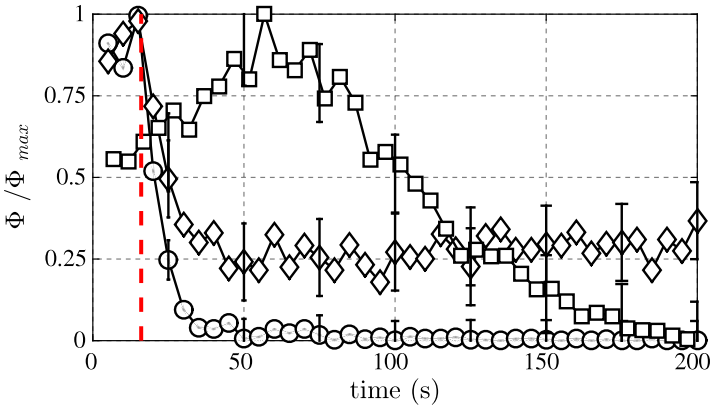

Fig. 6. Normalized evacuees flow rate ($\Phi/\Phi_{\max}$) vs. time. ◯ represent the "region 1" processes. ◊ represent the "region 2" processes. □ represent the "region 3" processes. The vertical red dashed line corresponds to the time stamp of maximum number of fallen pedestrians per unit time (see Fig. 5). Mean values were computed from (approx.) 120 realizations. The curves are normalized to have its maximum at unity. The error bars corresponds to $\pm\sigma$ (one standard deviation). The desired velocity was $v_d = 6$ m/s. (For interpretation of the references to color in this figure legend, the reader is referred to the web version of this article.)

in the evacuation process, with an uncertain ending time. The third situation (labeled as "region 3") actually finished when almost all of the individuals (beyond 150) left the room.

Fig. 5 shows the (mean) number of fallen pedestrians per unit time along the evacuation process for each qualitative region. Clearly, the maximum rate of fallen pedestrians occurs at the beginning of the evacuation process, say, at approximately 20 s. This is in agreement with the fact that high pressures should be present for at least 15 s before the individual becomes unconscious (see Section 3). Furthermore, Fig. 5 indicates that the pressure in the bulk surmounts the injury limit from the very beginning of the evacuation process. However, after the first 20 s, the rate of fallen individuals slows down, regardless of the locus where the process lies in Fig. 4. The qualitative different situations corresponding to the locus in Fig. 4 do not actually depend on the rate of unconsciousness. We also checked over that these situations do not depend on the total number of fallen individuals (roughly, 20 individuals in our simulations).

Besides the rate of fallen pedestrians, we analyzed the flow rate of surviving individuals. Fig. 6 exhibits the flow rate of the leaving pedestrians along time. Three data sets are shown, each one representing the mean flow value for each corresponding region in Fig. 4(a). A vertical dashed line (red in the on-line version) also represents the time when the maximum rate of fallen people occurs. Notice that the (mean) flow rate for the "region 3" processes is qualitatively different from the ones corresponding to the "region 1" and the "region 2" processes. The former has a positive slope until 50 s, while regions 1–2 have negative or null slopes. Therefore, the "region 3" processes manage to keep a high rate of people leaving the room, while the other two situations makes it harder (or even impossible) for the individuals to escape.

Fig. 6 also gives us a better understanding of Fig. 4(a) for the different behaviors between the "region 1" and "region 2" processes. Both situations have a diminishing flow rate, according to Fig. 6. But, the flow rate of the "region 2" processes is non-vanishing, although weak. The number of evacuees above 50 in "region 2" (see Fig. 4(a)) can be explained by the weak flow rate beyond 50 s appearing in Fig. 6. This is in agreement with the mentioned uncertainty in the ending time for

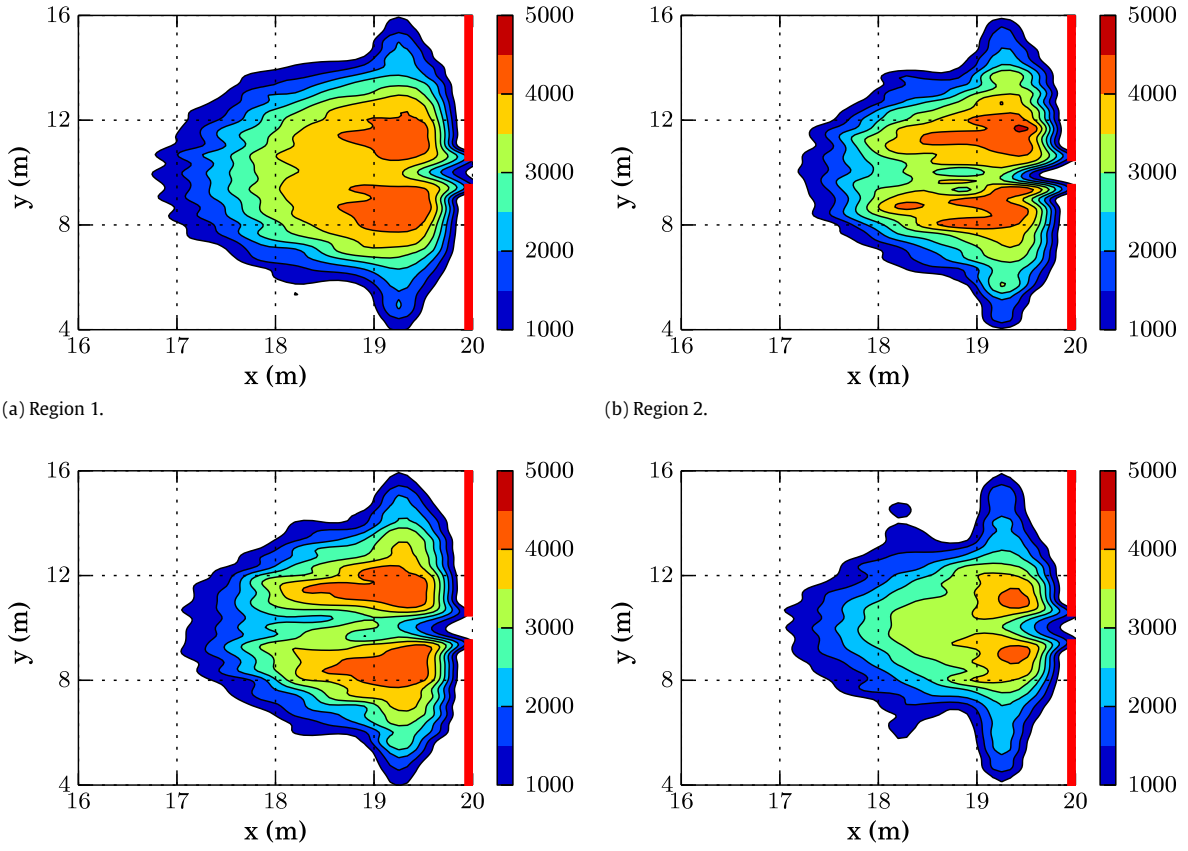

(a) Region 1.

(b) Region 2.

(c) Region 3.

(d) No fallen pedestrians.

Fig. 7. (Color on-line only) Mean social pressure contour lines computed from 30 evacuation processes for the first 100 s. Fig. 7(d) represent corresponds to evacuation processes with non fallen (unconscious) individuals. The scale bar on the right is expressed in N m^{-1} units (see text for details). We included the social pressure over both types of pedestrians (moving and fallen). The red lines at $x = 20$ m represent the walls on the right of the room. The pedestrian's desired velocity was $v_d = 6$ m/s. The contour lines were computed on a square grid of 1 m $\times$ 1 m and then splined to get smooth curves. Level colors can be seen in the on-line version only.

the "region 2" processes. On the contrary, the vanishing flow rate for the "region 1" processes means that the evacuation process finishes after a relatively short time period. Consequently, the expected t_{exit} is relatively low, as shown in Fig. 4(a).

A few conclusions can be outlined from the above analysis. For the dodging scenario (and high pressures) three situations appear to be possible. The first situation (*i.e.* "region 1" processes) occurs when the evacuation ceases in a short time period and a small fraction of the pedestrians are able to leave the room. The second situation (*i.e.* "region 2" processes) has a very similar performance as the first situation at the beginning of the process, but instead of ceasing after this time period, it "slows down", like a "leaking" process. The "slow down" seems endless because the "leaking" delays the evacuation to very long time periods. The third situation (*i.e.* "region 3" processes) corresponds to high flow rates, allowing a large fraction of the pedestrians to leave the room.

5.1.2. The social pressure for the dodging scenario

In Section 5.1.1 we analyzed the rate of fallen individuals and the flow rate of the outgoing pedestrians. As a second step in the investigation, we studied the pressure patterns inside the bulk for the three main loci represented in Fig. 4(a). The contour maps are shown in Fig. 7. It also includes the situation where the pedestrians are not allowed to become unconscious (see Fig. 7(d)). Notice that the contour maps include the pressure actuating on *all* the crowd (that is, either the conscious and unconscious pedestrians).

The higher pressure zones in all the contour maps appear on the sides of the exit (see Fig. 7). But the "region 1" processes (Fig. 7(a)) exhibit a qualitative difference in the middle of the room with respect to the other processes (Fig. 7(b) and (c)). The former shows a widely spread high pressure area centered at the mid-path $y = 10$ m. Instead, Fig. 7(b) and (c) show a low pressure path along $y = 10$ m.

Recall that the flow rate vanishes for the "region 1" situation. Thus, Fig. 7(a) represents the pressure map when the pedestrians are not able to leave the room. Notice that this pressure map is opposed to the one shown in Fig. 7(d) where

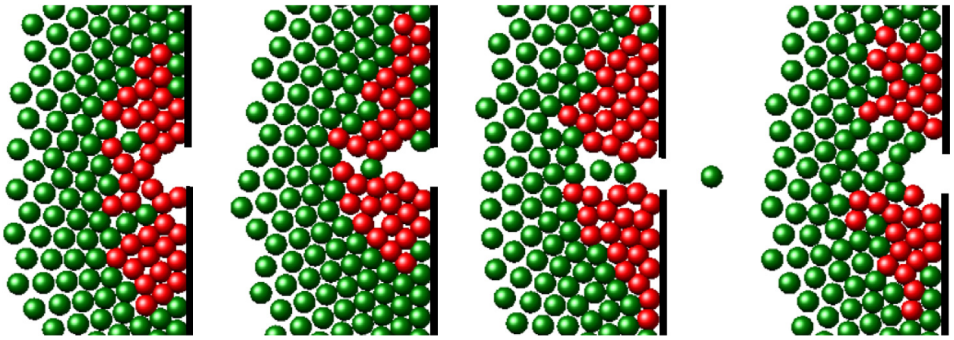

(a) Total blocking (region 1).

(b) Partial blocking (region 1).

(c) Narrow pathway (region 2).

(d) Wide pathway (region 3).

Fig. 8. (Color on-line only) Snapshots of different evacuation processes for each region in the first 100 s of the processes. Moving and fallen pedestrians are represents in green and red circles, respectively. The black lines represent the walls on the right of the room. The pedestrian's desired velocity was $v_d = 6$ m/s.

(all) non-unconscious pedestrians can manage to get out. This outgoing flow diminishes the bulk pressure, specially in the middle of the room (see Fig. 7(d)). See further details in Section 5.2.

The low pressure mid-path appearing in Fig. 7(b) and (c) can be associated to the non-vanishing pedestrian flow rates for "region 2" and "region 3", respectively. However, the "region 3" mid-path pattern resembles better the one with no unconscious pedestrians (see Fig. 7(d)). This fact suggests that the mid-path configuration is responsible for the performance differences between the "region 2" and the "region 3" situations.

The possible evacuation situations for the dodging scenario can be summarized as follows. The first situation (*i.e.* "region 1" processes) only allows the evacuation for a short time period after the rate of fallen pedestrians reaches a maximum. No low pressure paths remain open after the evacuation becomes frustrated. The low pressure paths only remain open (during long time periods) for the second and third situation (*i.e.* "region 2" and "region 3", respectively). However, some connection appears to exist between the evacuation performance of each situation and the path configuration. The third situation resembles better the evacuation processes with no unconscious pedestrians.

5.1.3. The evacuation pathway for the dodging scenario

Recall once again the process loci shown in Fig. 4(a). We examined separately the process animations for the three situations labeled as regions 1, 2 and 3. Fig. 8 shows four representative snapshots for these evacuation processes. The snapshots were recorded at 100 s, that is, at the stage where each situation can be differentiated easily.

Fig. 8(a) and (b) correspond to two representative snapshots for the "region 1" situation. The unconscious (fallen) pedestrians are blocking the exit in both pictures. However, only one blocking cluster appears in Fig. 8(a), while two blocking clusters can be seen in Fig. 8(b). These correspond to a *total* blocking situation and a *partial* blocking situation, respectively, as defined in Section 2.6. No pathway exists at all for the moving pedestrians to leave the room, in agreement with the corresponding (mean) flow rate shown in Fig. 5 and the contour map shown in Fig. 7(a).

Fig. 8(c) and (d) correspond to two representative snapshots for the "region 2" and "region 3" situations, respectively. Both situations exhibit an available pathway for the moving pedestrians to leave the room. This means that the outgoing flow is non-vanishing, as reported in Fig. 6. Thus, the snapshots confirm that a mid-path configuration is actually responsible for allowing the individuals to leave the room. The difference between Fig. 8(c) and (d) corresponds, however, to the pathway width. This path is approximately one pedestrian width (0.6 m) for the "region 2" situation, while it appears wider for the "region 3" situation. The contour maps in Fig. 7(b) and (c) resemble quite accurately this difference.

It is immediate that the wider the leaving pathway, the better evacuation performance. But a close examination of the animations for the "region 2" situation shows that the pedestrians leave the room intermittently, following a stop-and-go behavior. This is qualitatively different from the "region 3" situation, where more than one individual can leave the room almost simultaneously. The stop-and-go behavior is responsible for the regular flow in Fig. 6, resembling a "leaking-like" process. On the contrary, the "region 3" situation allows an increasing number of pedestrians to leave the room (see Fig. 6), until no more unlocked pedestrians are available in the room.

The above analysis from the snapshots and animations (not shown) summarizes as follows. The pedestrians located on the sides of the door experience the higher pressure in the bulk, and thus, have the higher probability to become unconscious. The unconscious (fallen) pedestrians may or may not block the exit. If a partial or total blocking occurs (as defined in Section 2.6), the outgoing flow immediately vanishes and the evacuation becomes frustrated. The "region 1" resembles this situation.

If the unconscious (fallen) pedestrians do not block the exit, the remaining pathway plays an important role. For narrow pathways (*i.e.* width close to 0.6 m), the overall evacuation slows down due to a stop-and-go dynamic along the pathway. For wider pathways, the individuals can manage to get out easily, and consequently, the evacuation process improves.

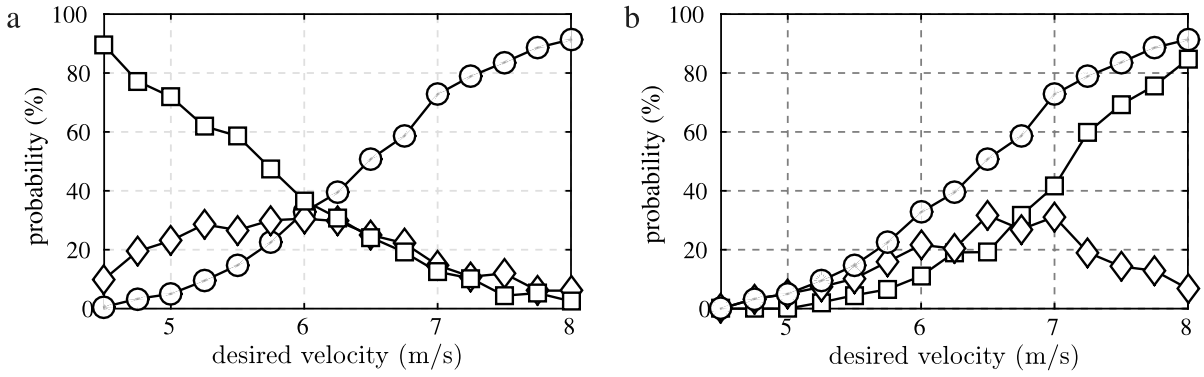

Fig. 9. (a) Probability for each type of evacuation process vs. desired velocity (anxiety level). ◯ represent the "region 1" processes (blocking). ◊ represent the "region 2" processes (narrow pathway). □ represent the "region 3" processes (wide pathway). (b) Contribution of each type of blocking to the total blocking probability of the exit vs. desired velocity (anxiety). ◯ represent the blocking probability of the exit. ◊ represent the partial blocking probability of the exit. □ represent the total blocking probability of the exit. All the probabilities were computed over 360 realizations (both plots). The simulated time period was 300 s.

5.1.4. The role of the desired velocity for the dodging scenario

We examined the dodging scenario for the desired velocity $v_d = 6$ m/s through Sections 5.1.1–5.1.3. We now vary the desired velocity from 4.5 to 8 m/s. For desired velocities below 4.5 m/s, no pedestrians become unconscious.

Fig. 9(a) shows the probability of attaining any of the three evacuation situations (*i.e.* regions 1, 2 or 3). We observe that the probability for the region 1 raises as the desired velocity increases, that is, as the individuals become more and more anxious. The region 3 processes decrease along the same interval of v_d. But, the region 2 situation achieves a maximum at 6 m/s. Notice that the three situations are equally likely only at 6 m/s. This is a nice anxiety level for equally sampling all the possible situations.

The blocking configuration of the "region 1" situation also changes as the desired velocity increases. Fig. 9(b) shows the *total* and *partial* blocking probability as a function of the desired velocity. The *total* blocking probability becomes relevant beyond $v_d = 7$ m/s with respect to the *partial* blocking probability. This means that all the moving pedestrians will be locked due to a barrier surrounding the exit (for our simulation conditions).

We conclude that the number of leaving pedestrians will depend on the desired velocity (*i.e.* anxiety level) of the individuals, according to our simulations (and for the current initial conditions). The desired velocity controls the probability of attaining any of the three possible situations, that is, the situations labeled as region 1, 2, or 3 (see Fig. 4(a)).

5.2. The passing-through scenario

We now assume a different behavioral pattern for the moving pedestrians: they are able to pass-through unconscious (fallen) individuals in order to get out of the room. They no longer dodge the fallen pedestrians, since we assume that the passing-through is always possible, regardless of the additional difficulty that implies this new dynamic (see Section 2.5 for details). In the Appendix we show how the parameters used in this Section were simulated.

Fig. 10(a) exhibits a snapshot of an evacuation process in the passing-through scenario. The overlapping individuals are actually the ones passing through unconscious (fallen) pedestrians. The processes loci for the passing-through scenario is shown in Fig. 10(b) for the desired velocity of $v_d = 6$ m/s and the passing-through velocity of $v_p = 0$ m/s. The null value of v_p means that the passing-through individual experiences a moving difficulty such that his (her) willing vanishes. The passing-through pedestrian actually moves forward due to the individuals pushing from behind.

A quick comparison between Figs. 4(a) and 10(b) shows that switching from the dodging scenario to the passing-through one shifts the "region 1" and "region 2" loci to the "region 3" location. Therefore, we realize that the passing-through dynamic enhances the evacuation performance for those situations where dodging achieves a narrow pathway, or, some kind of blocking (*i.e.* total or partial).

Notice that the "region 1" situation becomes relevant for $v_d > 6$ m/s, according to Fig. 9(a). This means that the evacuation enhancement will not be significant below this range. The same can be said about the "region 2" situation.

Since the passing-through dynamics improve the evacuation processes, we asked ourselves for the differences between this scenario and the one with non-unconscious pedestrians. That is, we investigated how similar could both scenarios be. Fig. 11 exhibit the flow rates and mean pressures for both scenarios.

Fig. 11 exhibit the flow rates and mean pressures for both scenarios. The pressure patterns in Fig. 11(a) and (c) correspond to the passing-through and non-unconscious scenarios, respectively. Both patterns look very similar for the first 100 s (roughly, the first half of the process), but somehow differentiate beyond this interval. The social pressure for the non-unconscious scenario decreases sharply until vanishing at 150 s. On the contrary, the passing-through scenario does not

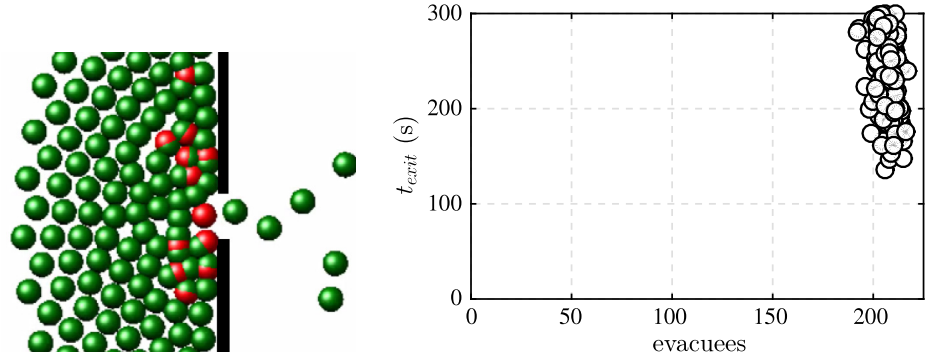

(a) Snapshot ($v_p = 0$ m/s). (b) Passing-through ($v_p = 0$ m/s).

Fig. 10. (a) (Color on-line only) Snapshot of an evacuation process at 100 s. Moving and fallen pedestrians are represented in green and red circles, respectively. The black lines represent the walls on the right of the room. The pedestrian's desired velocity was $v_d = 6$ m/s and the passing-through velocity was $v_p = 0$ m/s. (b) Leaving time t_{exit} of the last evacuee as a function of the number of evacuees. Each circle represents an evacuation process (360 processes are actually represented). All the evacuation processes were recorded along the first 300 s. The desired velocity was $v_d = 6$ m/s and the passing-through velocity was $v_p = 0$ m/s.

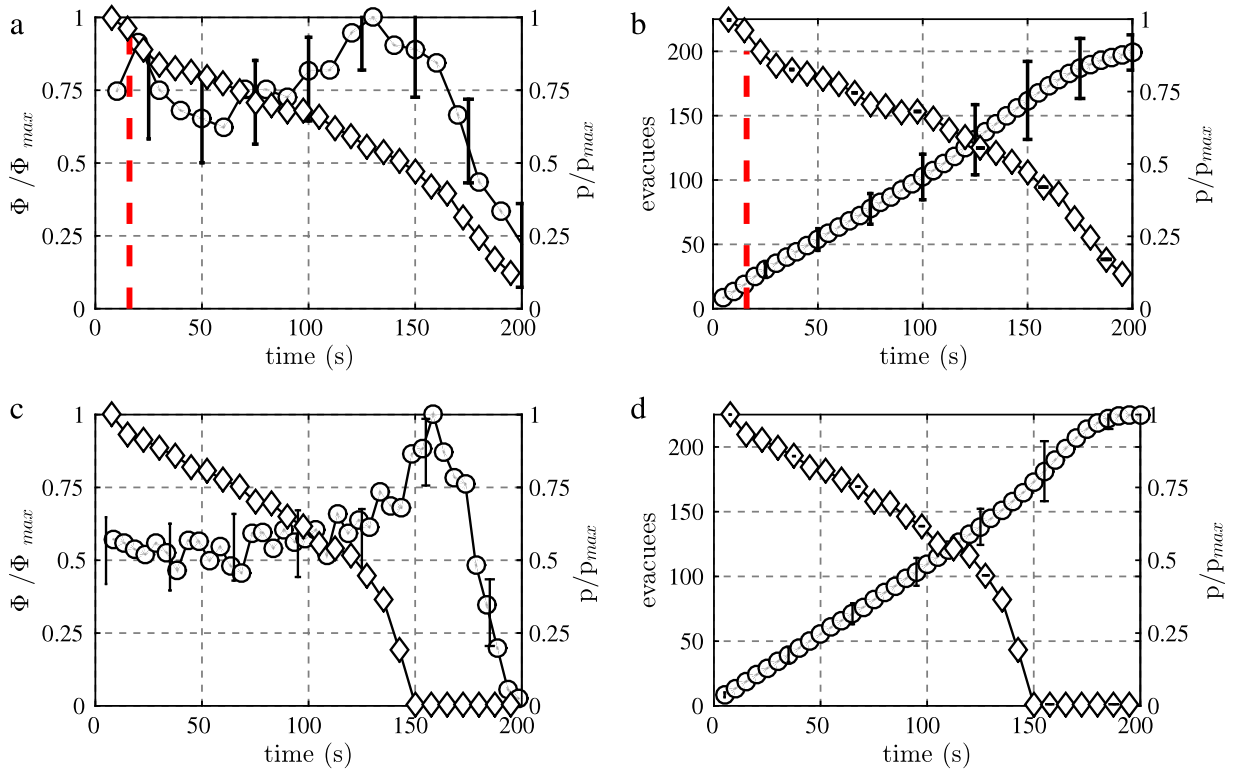

Fig. 11. (Color on-line only) The (a) and (b) plots correspond to the passing-through scenario with passing-through velocity $v_p = 0$ m/s. The (c) and (d) plots correspond to the non-unconscious pedestrian scenario. The vertical red dashed line corresponds to the time stamp for the maximum number of fallen pedestrians per unit time (see Fig. 5). For (a) and (c) plots: ◯ represent the normalized evacuees flow rate ($\Phi/\Phi_{\max}$) and ◊ represent the normalized mean social pressure ($p/p_{\max}$) vs. time. For (b) and (d) plots: □ represent the number of evacuees and ◊ represent the normalized mean social pressure ($p/p_{\max}$) vs. time. Mean values were computed from 50 realizations. Only the moving pedestrian contributed to the mean social pressure computation in (a) and (b) plots. The curves were normalized to have its maximum at unity. The error bars corresponds to $\pm\sigma$ (one standard deviation). The desired velocity was $v_d = 6$ m/s.

vanish, but diminishes to a lower level. This level corresponds to the pressure on the pedestrians that are not able to get out, since their passing-through velocity is null ($v_p = 0$).

The flow rate patterns represented in Fig. 11(a) and (c) are also quite similar. The (normalized) flow rate for the passing-through scenario appears higher than the one for the non-unconscious scenario because the former does not present a sharp maximum close to 150 s as the latter. This is in agreement with the vanishing pressure shown in Fig. 11(c). That is, no individuals remain locked behind any unconscious pedestrian, and thus, pressure can be completely released.

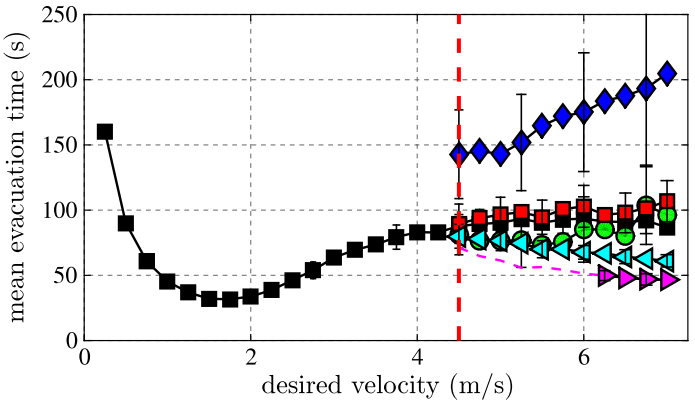

Fig. 12. (Color on-line only) Mean evacuation time for 100 individuals as a function of the desired velocity. ■ No fallen pedestrians ("faster is slower"); ◆ Narrow pathway; ■ Wide pathway; ● $v_p = 1$ m/s; ◀ $v_p = 3$ m/s; ▶ $v_p = 6$ m/s ($v_p < v_d$); ▪▪▪ limit between those situations with no fallen (unconscious) individuals and thew ones with fallen pedestrians; mean values were computed from 30 realizations; the error bars corresponds to $\pm\sigma$ (one standard deviation).

We conclude from Fig. 11 that, although the passing-through and non-unconscious scenarios correspond to qualitatively different dynamics, the overall evacuation performance is quite similar for the null passing-through velocity ($v_p = 0$). The only noticeable difference corresponds to those individuals that cannot manage to leave the room because of unconsciousness or null passing-through velocity $v_p = 0$.

We finally compared the overall performance for the different scenarios, as shown in Fig. 12. The evacuation time in Fig. 12 corresponds to the time interval until 100 individuals leave the room, in order to include the slow processes from the "region 2" situation. Notice that the unconscious (fallen) scenario data points lie beyond $v_d = 4.5$ m/s since there are no fallen individuals for lower desired velocities.

According to Fig. 12, the "region 3" situation does not actually improve the evacuation with respect to the non-unconscious scenario for the first 100 pedestrians leaving the room. But, the passing-through dynamics improves the evacuation performance for increasing values of v_p. Recall that v_p regulates the difficulty experienced by the pedestrians passing through unconscious individuals. As v_p increases, his (her) willing gets stronger because the degree of difficulty is supposed to diminish.

A brief summary for the evacuation performance in the two investigated contexts can be expressed as follows: the dodging scenario may worsen the evacuation performance with respect to the non-unconscious scenario, but, the passing-through scenario may improve the evacuation performance with respect to the same non-unconscious scenario. Both cases, the worsening or the enhancement, occur under certain conditions only. We were able to identify the desired velocity v_d and the passing-through willing v_p as two relevant control parameters for achieving this changes (for the setting mentioned in Section 4.1). The worsening becomes noticeable for desired velocity $v_d > 6$ m/s. Besides, the enhancement becomes noticeable for passing-through willings $v_p > 3$ m/s.

6. Conclusions

Our research focused on the high pressure scenarios during an emergency evacuation. Pressure is responsible for asphyxia and unconsciousness during the evacuation. People may fall, while others will further manage to escape. Two opposed scenarios are likely to happen: the moving pedestrians dodge the unconscious individuals, or, they manage to pass through them. In order to face these scenarios in the context of the "social force model", we *hypothesized* that a "passing-through" force may be present or not, in order to attain either one scenario or the other. We stress that this is a *first approach* to the aforementioned scenarios.

According to our simulations, unconsciousness is more likely to occur on the sides of the exit. For this reason, the unconscious (fallen) individuals not always block the exit completely. We arrived to the unexpected conclusion within this model that neither the number of unconscious (fallen) pedestrians nor the falling rate of these individuals are relevant for the probability of blocking the exit. This conclusion holds for a fixed desired velocity $v_d = 6$ m/s.

We first focused on the dodging scenario. This scenario *assumes* that moving pedestrians *always* dodge the unconscious (fallen) individuals. As opposed to the "passing-through" scenario, the evacuation performance strongly depends on how the unconscious (fallen) individuals group into clusters. Our research was able to distinguish between those situations that block the exit, and the ones where a free pathway remains open. The pathway width was found to be relevant for the evacuation performance, in agreement with experimental data reported in the literature. Therefore, three situations were well established: the blocking (totally or partially) situation, the narrow pathway situation (roughly, one individual's diameter) and the wide pathway situation. The overall performance of the dodging scenario depends on the probability of attaining any of these three possible situations.

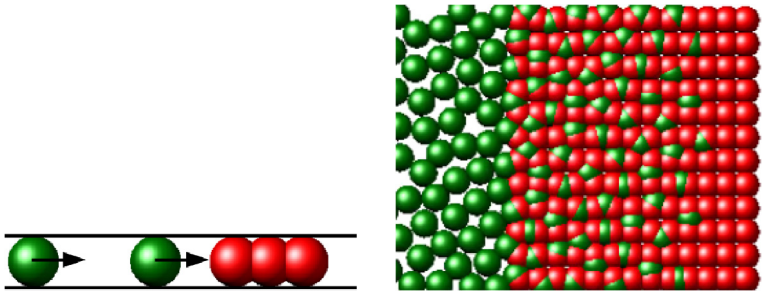

(a) Single lane. (b) Multiple lanes.

Fig. A.13. (Color on-line only) Snapshots of different evacuation processes used to study the effects over the pedestrians that pass through the fallen individuals. Moving and fallen pedestrians are represent in green and red circles, respectively. The pedestrian's desired velocity was $v_d = 6$ m/s and the pass through velocity was $v_p = 1$ m/s. (a) Narrow corridor with two moving pedestrians and three fallen individuals. The arrows represent the direction of the desired velocity. The black lines represent the walls of the corridor. (b) Wide corridor (5.5 m of width) with 135 moving pedestrians and 155 fallen individuals. The moving direction is from left to right.

We acknowledged that the evacuation process becomes interrupted after a short time period for the blocking situation. This is the worst situation, since many pedestrians get locked in the room because of the blocking clusters. On the contrary, if the grouping of unconscious (fallen) pedestrians allows a wide pathway to remain open, the dodging scenario does not show a significant worsening with respect to the lack of unconscious pedestrians.

The most interesting effect was captured for the narrow pathway situation. The moving pedestrians were only able to leave the room one after the other, in a stop-and-go process. This is a novel result and explains the significant slowing down that occurs for some processes in the dodging scenario. Experimental support for this kind of results can be found in the references mentioned in Section 1.

Our investigation on the dodging scenario explored a wide range of desired velocities, that is, we varied the anxiety level of the pedestrians. We specifically examined the range $4\,\mathrm{m/s} < v_d < 8\,\mathrm{m/s}$. We concluded that the probability for the wide pathway situation was only relevant along the lower half of this range. Instead, the blocking situation became relevant for the upper half. The narrow path situation was relevant only around $v_d = 6$ m/s. All these conclusions showed that the desired velocity (or anxiety level of the pedestrians) is a control parameter for attaining any of the three possible situations. This is valid for the fixed initial conditions detailed in Section 4.1.

We secondly focused on the "passing-through" scenario. Recall that we postulated the existence of a "passing-through" force in order to achieve a *first approach* to this problem. In this context, the pedestrian that passes through a fallen individual overcomes any blocking, although the difficulties, since the other pedestrians pushing from behind makes him move forward. Therefore, the overall evacuation performance improves with respect to the dodging scenario. Our investigation shows, however, that the passing-through willings need to surpass certain threshold (say, $v_p > 3$ m/s) for the improvement to become noticeable.

Acknowledgments

C.O. Dorso is a main researcher of the National Scientific and Technical Research Council (spanish: Consejo Nacional de Investigaciones Científicas y Técnicas—CONICET), Argentina, and full professor at Departamento de Física, Universidad de Buenos Aires. G.A. Frank is an assistant researcher of the CONICET, Argentina. F.E. Cornes has degree in Physics.

Appendix. Lanes of unconscious pedestrian

This appendix examines the behavior of one or more lanes of pedestrians willing to pass through unconscious (fallen) individuals. The "passing-through" pedestrians move from left to right. The unconscious pedestrians are grouped in a compact cluster, located in the way of the "passing-through" pedestrians. Two situations follow: the single lane situation and the multiple lane situation.

A.1. The single lane situation

The most simple process that we can imagine corresponds to a single pedestrian passing through a small group of unconscious (fallen) individuals, as shown in Fig. A.13(a).

The "passing-through" pedestrian does not experience a social repulsive force due to the unconscious individuals, but the willing of passing through them v_p. Thus, solving Eq. (1) for this process arrives to the expressions

$$\begin{cases} v &= v_p + (v_d - v_p)\, e^{-(t-t_0)/\tau'} \\ x &= x_0 - \tau' \left[v - v_d + v_p \, \ln\left(\dfrac{v_p - v}{v_p - v_d} \right) \right] \end{cases} \tag{A.1}$$

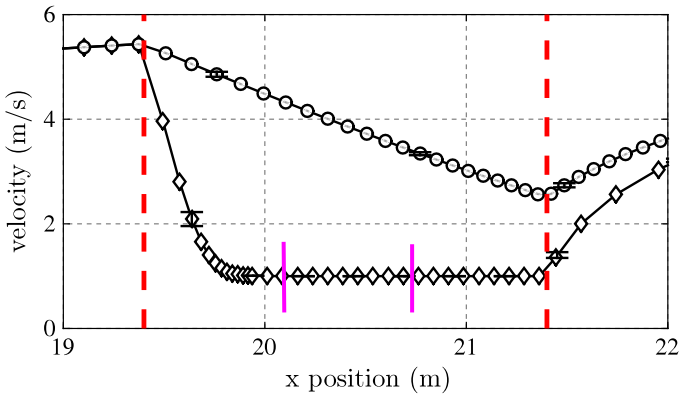

Fig. A.14. Velocity of a pedestrian through a lane of three fallen individuals. ◯ represent a reaction time of $\tau' = 0.5$ s (corresponds to the basic social force model). ◊ represent a reaction time of $\tau' = 0.05$ s. Mean values were computed from 30 realizations. The error bars corresponds to $\pm\sigma$ (one standard deviation). The vertical red dashed lines represent the initial and the ending positions of the fallen pedestrian's lane. The vertical magenta solid line represents the initial and the ending position of each fallen pedestrian. The individual moves free until the lane of fallen pedestrian. The pedestrian's desired velocity was set to $v_d = 6$ m/s, while the passing-through velocity was set to $v_p = 1$ m/s. (For interpretation of the references to color in this figure legend, the reader is referred to the web version of this article.)

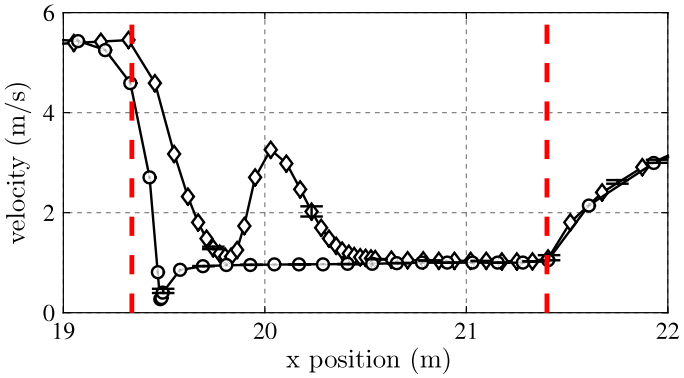

Fig. A.15. Velocity of two pedestrians through the lane of three fallen individuals. The value of τ' was 0.05 s. ◊ represent the first individual to reach the lane of fallen pedestrians. ◯ represent the second individual that reaches lane of fallen pedestrians (the left most moving pedestrian). Mean values were computed from 30 realizations. The error bars correspond to $\pm\sigma$ (one standard deviation). The vertical red dashed lines represent the initial and the ending positions of the lane of fallen pedestrians. The individuals moves freely until they reach the lane of fallen pedestrians. The pedestrian's desired velocity was $v_d = 6$ m/s and the passing-through velocity was $v_p = 1$ m/s. (For interpretation of the references to color in this figure legend, the reader is referred to the web version of this article.)

for the initial conditions $x(t_0) = x_0$ and $v(t_0) = v_d$. The latter expresses that the pedestrian is moving freely before reaching the first unconscious (fallen) individual at position x_0 and time t_0. Fig. A.14 is a simulation of Eq. (A.1) for two different values of τ'.

Notice from Fig. A.14 that a passing-through relaxation time of $\tau' = 0.5$ s is too long for the pedestrian to reach the passing-through velocity v_p within the distance of the first fallen individual (that is, 0.6 m). But, reducing the relaxation time value to roughly 10% accelerates the process, in order to reach v_p within the expected distance. Thus, the value $\tau' = 0.05$ s is now meaningful, according to the definition given in Section 2.5. Recall that this is a *first approach* for the passing-through dynamics.

The willing for passing through unconscious (fallen) pedestrians is regulated by the passing-through velocity v_p. There is currently no experimental value for v_p in the literature to our knowledge. But, v_p represents a slowing down in v_d due to the difficulties of the "passing-through" context (see Section 2.5). We fixed $v_p = 1$ m/s in Fig. A.14 as a first example. Other possible values can be found in Section 5.2.

We further included a second pedestrian passing through the lane, as shown in Fig. A.13(a). Both moving pedestrians pass through the unconscious individuals, one after the other. Fig. A.15 exhibits their velocity profiles as a function of the position.

The velocity profile in Fig. A.15 for the first pedestrian passing through the unconscious (fallen) individuals differs from the profile in Fig. A.14. There is a maximum velocity immediately after the initial position of the lane (red line in Fig. A.15). This maximum corresponds to the pushing effect of the pedestrian behind him (her). Thus, our model for passing through unconscious individuals succeeds in capturing the effect of "pushing from behind". Furthermore, this pushing effect allows

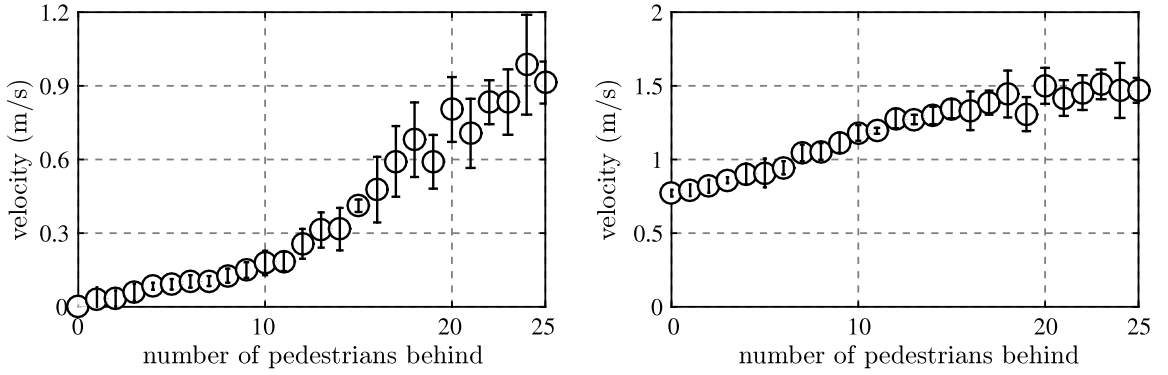

(a) $v_p = 0$ m/s. (b) $v_p = 1$ m/s.

Fig. A.16. Mean velocity per individual as a function of the number of pedestrians behind him (her). Mean values were computed from 30 realizations. The error bars corresponds to $\pm\sigma$ (one standard deviation). The pedestrian's desired velocity was $v_d = 6$ m/s.

the moving pedestrians to pass through the unconscious individuals even though $v_p = 0$ m/s. That is, if the passing-through pedestrian experiences a moving difficulty such that his (her) willing vanishes.

Notice in Fig. A.15 that the second pedestrians slows down immediately after entering the unconscious zone. This is the counterpart effect of "pushing from behind".

A.2. The multiple lane situation

We introduced a multiple lane situation in order to deep into the "pushing from behind" and the "slowing down" effects. As shown in Fig. A.13(b), an arrangement of 12×13 unconscious (fallen) individuals was placed at the right of 135 moving pedestrians. The moving pedestrians had the desire to go to the right. We simulated two situations: the pedestrian's passing-through velocity was null ($v_p = 0$ m/s), or, the passing-through velocity was $v_p = 1$ m/s. The former corresponds to pedestrians experiencing greater difficulties to surpass the unconscious individuals than the latter. Fig. A.16 shows the mean velocity of the moving pedestrians as a function of the number of pushing people from behind (see caption for details).

Fig. A.16(a) exhibits a null velocity if there are no other pushing pedestrians behind him (her). This is right, since the surpassing difficulties resembles a vanishing willing ($v_p = 0$ m/s). But, as more people push from behind, his (mean) velocity increases. For 25 pushing pedestrians, the mean velocity is close to 1 m/s.

Fig. A.16(b) exhibits a mean velocity below 1 m/s if there are no pedestrians pushing from behind. This is less than v_p and corresponds to the "slowing down" due to the pedestrians in front of him (that is, at the right of his current position). Notice that the "slowing down" diminishes as more people push from behind. At some point, both effects (the "slowing down" and the "pushing") balance and the mean velocity becomes similar to $v_p = 1$ m/s. For 25 pushing pedestrians, the mean velocity of the passing-through individuals converges to 1.5 m/s. This value is in agreement with the measured velocity of the single individual in Fig. A.15. That is, from Fig. A.15 we can expect a mean value between 1 and 2 m/s. It also confirms that the "slowing down" is no longer relevant when 25 individuals push from behind.

References

[1] J. Fruin, The causes and prevention of crowd disasters, in: R. Smith, J. Dickie (Eds.), Engineering for Crowd Safety, Elsevier Science Publishers BV, 1993, pp. 1–10.
[2] CrowdsafeDatabase maintained by Crowd Management Strategies.
[3] W. Daamen, S.P. Hoogendoorn, Emergency door capacity: Influence of door width, population composition and stress level, Fire Technol. 48 (1) (2012) 55–71. http://dx.doi.org/10.1007/s10694-010-0202-9.
[4] A. Seyfried, B. Steffen, A. Winkens, T. Rupprecht, M. Boltes, W. Klingsch, Empirical Data for Pedestrian Flow Through Bottlenecks, Springer Berlin, Heidelberg, Berlin, Heidelberg, 2009, pp. 189–199.
[5] W. Liao, A. Seyfried, J. Zhang, M. Boltes, X. Zheng, Y. Zhao, Experimental study on Pedestrian flow through wide bottleneck, Trans. Res. Procedia 2 (2014) 26–33. http://dx.doi.org/10.1016/j.trpro.2014.09.005.
[6] R. Nagai, M. Fukamachi, T. Nagatani, Evacuation of crawlers and walkers from corridor through an exit, Physica A 367 (2006) 449–460. http://dx.doi.org/10.1016/j.physa.2005.11.031.
[7] G.A. Frank, C.O. Dorso, Evacuation under limited visibility, Internat. J. Modern Phys. C 26 (01) (2015) 1550005. http://dx.doi.org/10.1142/S0129183115500059.
[8] G.A. Frank, C.O. Dorso, Panic evacuation of single Pedestrians and couples, Internat. J. Modern Phys. C 27 (08) (2016) 1650091. http://dx.doi.org/10.1142/S0129183116500911.
[9] A. Garcimartn, D.R. Parisi, J.M. Pastor, C. Martn-Gmez, I. Zuriguel, Flow of Pedestrians through narrow doors with different competitiveness, J. Stat. Mech. Theory Exp. 2016 (4) (2016) 043402.
[10] A. Schadschneider, W. Klingsch, H. Klüpfel, T. Kretz, C. Rogsch, A. Seyfried, Evacuation Dynamics: Empirical Results, Modeling and Applications, Springer New York, New York, NY, 2009, pp. 3142–3176.
[11] R.S. Lee, R.L. Hughes, Prediction of human crowd pressures, Accid. Anal. Prev. 38 (4) (2006) 712–722.
[12] J. Gill, K. Landi, Traumatic asphyxial deaths due to an uncontrolled crowd, Am. J. Forensic Med. Pathol. 25 (2004) 358–361.
[13] D. Helbing, I. Farkas, T. Vicsek, Simulating dynamical features of escape panic, Nature (2000).

[14] G. Frank, C. Dorso, Room evacuation in the presence of an obstacle, Physica A 390 (11) (2011) 2135–2145.
[15] D. Helbing, P. Molnár, Social force model for Pedestrian dynamics, Phys. Rev. E 51 (1995) 4282–4286. http://dx.doi.org/10.1103/PhysRevE.51.4282.
[16] D. Parisi, C. Dorso, Microscopic dynamics of Pedestrian evacuation, Physica A 354 (2005) 606–618.
[17] S. Ødegaard, J. Kramer-Johansen, A. Bromley, H. Myklebust, J. Nysaether, L. Wik, P.A. Steen, Chest compressions by ambulance personnel on chests with variable stiffness: Abilities and attitudes, Resuscitation 74 (1) (2007) 127–134. http://dx.doi.org/10.1016/j.resuscitation.2006.12.006.
[18] A. Neurauter, J. Nysaether, J. Kramer-Johansen, J. Eilevstjønn, P. Paal, H. Myklebust, V. Wenzel, K.H. Lindner, W. Schmölz, M. Pytte, P.A. Steen, H.-U. Strohmenger, Comparison of mechanical characteristics of the human and porcine chest during cardiopulmonary resuscitation, Resuscitation 80 (4) (2009) 463–469. http://dx.doi.org/10.1016/j.resuscitation.2008.12.014.
[19] D. Parisi, C. Dorso, Morphological and dynamical aspects of the room evacuation process, Physica A 385 (1) (2007) 343–355.
[20] Claire C. Gordon, Thomas Churchill, Charles E. Clauser, Bruce Bradtmiller, John T. McConville, Ilse Tebbetts, Robert A. Walker, Anthropometric survey of US army personnel: summary statistics interim report, Tech. Rep., 1989.
[21] E. Evans, F. Hayden, Tests on live subjects to determine the tolerable force that may be exerted by crowd control crush barriers, Tech. Rep., University of Surrey, Department of Biomechanics, 1971.
[22] P. Tikuisis, P. Meunier, C. Jubenville, Human body surface area: measurement and prediction using three dimensional body scans, Eur. J. Appl. Physiol. 85 (3) (2001) 264–271. http://dx.doi.org/10.1007/s004210100484.
[23] R.L. Huston, Principles of Biomechanics, CRC Press, Taylor & Francis Group, 6000 Broken Sound Parkway NW, Suite 300, Boca Raton, FL 33487-2742, 2009.
[24] P.H.I.H.G. Hopkins, S.J. Pountney, M. Sheppard, Crowd pressure monitoring, in: R. Smith, J. Dickie (Eds.), Engineering for Crowd Safety, Elsevier Science Publishers BV, 1993, pp. 389–398.
[25] M. Mysen, S. Berntsen, P. Nafstad, P.G. Schild, Occupancy density and benefits of demand-controlled ventilation in Norwegian primary schools, Energy Build. 37 (12) (2005) 1234–1240. http://dx.doi.org/10.1016/j.enbuild.2005.01.003.
[26] S. Plimpton, Fast parallel algorithms for short-range molecular dynamics, J. Comput. Phys. 117 (1) (1995) 1–19. http://dx.doi.org/10.1006/jcph.1995.1039.